

Synthesized and characterization of calcium alginate beads as biosorbent of pollutants dye and phosphate from aqueous solution

S. Ben Ayed^a, L. Aloui^b, L. Mansour^c, F. Ayari^{a,*}

^aFaculty of Sciences of Bizerte, LR 05/ES09 Laboratory of Applications of Chemistry to Resources and Natural Substances and to the Environment (LACReSNE), Carthage University, Zarzouna 7021, Tunisia, emails: fadhilaayari@yahoo.fr (F. Ayari) ORCID ID: 0000-0002-3836-2029, sirinebenayed19@gmail.com (S. Ben Ayed)

^bAix-Marseille University, CNRS, MADIREL UMR 7246, 13397 Marseille Cedex 20, France, email: lobna.chimie@gmail.com

^cDepartment of Zoology, College of Science, King Saud University, P.O. Box: 2455, Riyadh 11451, Saudi Arabia, email: lmansour@ksu.edu.sa

Received 28 May 2023; Accepted 17 October 2023

ABSTRACT

In this study, we employed sodium alginate, a naturally occurring biodegradable biopolymer, to create calcium alginate beads through the cross-linking process using CaCl_2 as the gelling agent. The obtained beads were subjected to characterization through various analyses, including textural and structural structure via N_2 adsorption/desorption isotherm via Brunauer–Emmett–Teller method, Fourier-transform infrared spectroscopy, X-ray diffraction, and UV-Visible diffuse reflectance analyses. The effectiveness of this adsorbent was investigated in the removal of Auramine O dye (AO) and phosphate from aqueous solutions through an adsorption process. An initial examination of Auramine O and phosphate removal using calcium alginate beads as the adsorbent was conducted to identify the optimal adsorption conditions, including contact time (adsorbate/adsorbent), initial adsorbate concentration, pH, and initial adsorbent quantity. A full factorial design matrix was used to study the direct effects and interactions of the principal parameters. Experimental results show that under the optimal conditions, calcium alginate beads demonstrate significant adsorption capabilities, achieving a phosphate removal rate of 82.5% and an AO dye removal rate of 48% within a 180 min timeframe. The adsorption findings closely align with the Langmuir model in the case of Auramine O and the Freundlich model for phosphate indicating monolayer and multi-layer adsorption process, respectively. Moreover, the pseudo-second-order model fits effectively for both AO and phosphate, indicating a chemisorption process.

Keywords: Calcium alginate beads; Characterization; Pollutants; Adsorption; Optimization

1. Introduction

One of the most crucial and serious issues that human being have to confront as a result of the technology revolution is environmental pollution [1].

Toxic contaminants existing in the surface and ground water; for example, synthetic dyes have a harmful impact on human, plants and aquatic lives. Moreover, a recent

research of Klaus Hunge [2] reviewed different research focused on the use of Auramine O with various application such as textile, paper, plastic, gasoline and cosmetic industries. It may act as carcinogenic and mutagenic due to its bio-conversion to reactive species in target organs of rats and humans as well according to the International Agency for Research on Cancer [3,4]. Thus, it is essential to apply a treatment process for effluents that contain dyes treatment before discharged into the environment.

* Corresponding author.

On the other side, phosphates are very important materials that used also in many industrial applications such as detergents and fertilizers products fabrication, food manufacture and in the preparation of foodstuffs. This excessive use of phosphates leads to a huge amount of phosphate-bearing waste production that will be disposal to the environment as effluents [5]. This abundant amount of phosphates in the environment can cause the well-known phenomenon “eutrophication” that can cause the ecological degradation of water as a result of the growth of some harmful aquatic plants. To avoid this serious problem the removal of phosphates from water is necessary.

Adsorption is a technique that proved itself as one of the most efficient processes used in the removal of contaminants from water and wastewater [6]. Furthermore, the utilization of an eco-friendly, low cost and abundant material such alginate will add more attractiveness to the process. Alginate is a natural polysaccharide extracted from brown algae namely *Laminaria digitata* [7]. This biopolymer composed of α -(1→4)-linked l-guluronic acid (G) and β -(1→4)-linked d-mannuronic acid (M) units with different G:M ratio [8].

The gelation and ion binding properties of sodium alginate is mainly depend on the exchange of Na^+ ions from the guluronic acid unit with different multivalent metal cations (Ca^{2+} , Zn^{2+} , Sr^{2+} , Ba^{2+} , Al^{3+} etc.) to form a network cross-linked hydrogel structure called “egg-boxes” [8,9]. Calcium chloride was used in this work as the gelling agent because of its nontoxic nature and its inexpensiveness [10].

The main goal of this research is to remove phosphate and Auramine O dye from aqueous solution by adsorption onto calcium alginate beads as a green adsorbent since that a limited number of scientific papers have dealing with that and to study the impact of the key process parameters using a full factorial design matrix.

2. Materials and methods

2.1. Materials

The solutions in this study were formulated using distilled water, Auramine O (AO) ($\text{C}_{17}\text{H}_{21}\text{N}_3\text{Cl}$, molecular weight = 303.83 g/mol, maximum absorption wavelength $\lambda_{\text{max}} = 432$ nm), and potassium dihydrogen phosphate (KH_2PO_4 , molecular weight = 136.086 g/mol) obtained from Sigma-Aldrich. Fig. 1 depicts the structure of the AO dye. It is worth noting that all the chemicals employed in the adsorption experiments were of analytical reagent grade.

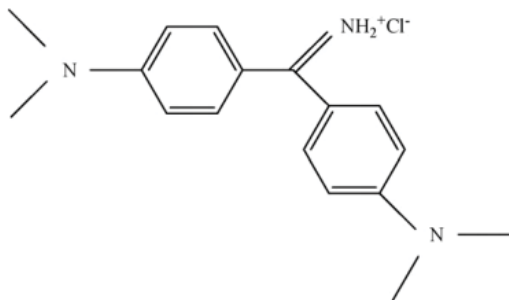


Fig. 1. Molecular structure of Auramine O dye.

pH adjustments were carried out using either 0.1 M HCl for acidic conditions or 0.1 M NaOH for alkaline conditions.

2.2. Preparation of calcium alginate beads

Two grams of sodium alginate powder was dissolved in 100 mL of deionised water with stirring for 60 min in order to get homogenous solution. This prepared mixture was then slowly added drop by drop into a 0.1 M calcium chloride solution using a syringe, resulting in the formation of calcium alginate beads. These beads, initially water-soluble due to the presence of sodium alginate, underwent a transformation into water-insoluble calcium alginate beads. The obtained beads were left in the solution for 24 h (curing time) to ensure the completion of the gelling reaction. In order to remove the remaining amount of non reacted calcium ions from the bead surfaces, all beads were washed several times with deionised water. Finally, the obtained beads can be used directly as wet calcium alginate beads (WA) (Fig. 2a), or after drying step at 60°C overnight in an oven and used as dry calcium alginate beads (DA) (Fig. 2b).

2.3. Batch adsorption experiments

Sorption experiments were studied in a batch mode under orbital stirring using Erlenmeyer flasks at room temperature. Dye solution was prepared by mixing 50 mL of AO ($[\text{AO}]_{\text{initial}} = 5$ mg/L) with 0.1 g of calcium alginate beads. For phosphate solution, 10 mg/L of phosphate was mixed with 1.5 g of adsorbent. The pH levels of each solution are carefully measured before and after the adsorption process, served in the assessment and understanding of the adsorption mechanism. To ensure the precision of the procedure, all experiments were conducted twice. Following the mixing of solutions, they were subjected to centrifugation at 4,000 tr/min (rpm), and the dye concentration in the resulting supernatant was determined by measuring the absorbance at $\lambda_{\text{max}} = 432$ nm using a UV-Vis spectrophotometer. The quantification of phosphate in the aqueous solution was performed utilizing the UV-spectrophotometric technique [11].

Pollutant removal percentage can be given by Eq. (1):

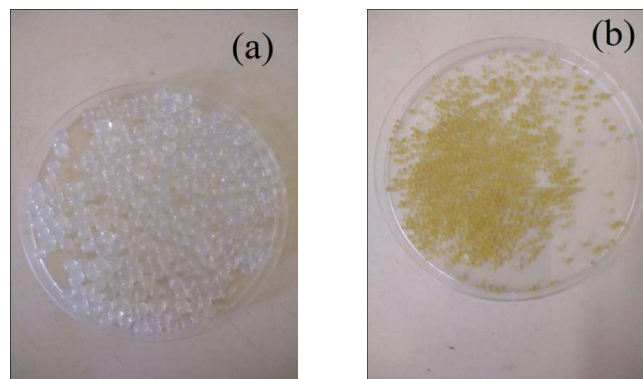


Fig. 2. Digital photographs of calcium alginate beads: (a) wet and (b) dry beads.

$$Y\% = \frac{C_0 - C_e}{C_0} \quad (1)$$

where C_0 : the initial concentration of the pollutant (mol/L or mg/L); C_e : the equilibrium concentration of the pollutant (mol/L or mg/L).

2.4. Characterization of alginate calcium beads

Powder X-ray diffraction using a PANalytical X'Pert HighScore Plus diffractometer (France), with monochromatic Cu-K radiation source ($\lambda = 1.5418 \text{ \AA}$) operated at 40 kV and 40 mA and Fourier-transform infrared spectroscopy (FTIR) model spectrum 100 (PerkinElmer, Waltham, Massachusetts, United States) in the range between 400–4,000 cm^{-1} were used to investigate the chemical structure of the obtained alginate beads. The N_2 adsorption–desorption isotherms, specific surface area (S_{BET}), total pore volume (V_t) and other porosity characteristics of the adsorbent were measured using a Quantachrome Model Nova 1000e (Germany) at

liquid nitrogen temperature of 77K. UV-Vis diffuse reflectance analysis was done using UV-Visible spectrophotometer (Shimadzu UV-2700, France).

3. Results and discussion

The FTIR spectrum (Fig. 3a) shows a broad band at 3,290 cm^{-1} assigned to O–H hydroxyl group of the alginate due the existence of the phenolic group [12]. The characteristic peak at 2,970 cm^{-1} can be attributed to aliphatic C–H stretching vibrations existing in alginate chain [13]. Both bands at 1,900 and 1,410 cm^{-1} are related to asymmetric and symmetric stretching vibrations of C(=O)OH ion of the biopolymer, respectively, while the antisymmetric stretching vibrations of C–O–C is served at 1,020 cm^{-1} [14]. Bands at 1,590 and 1,089 cm^{-1} are associated to the –COOH stretching vibration and –C–O stretching vibrations of this polysaccharide, respectively [13,15]. As we can see from X-ray diffraction (XRD) pattern of the calcium alginate beads (Fig. 3c), no peak has been appeared which proves the amorphous state formation of the material. The result is in

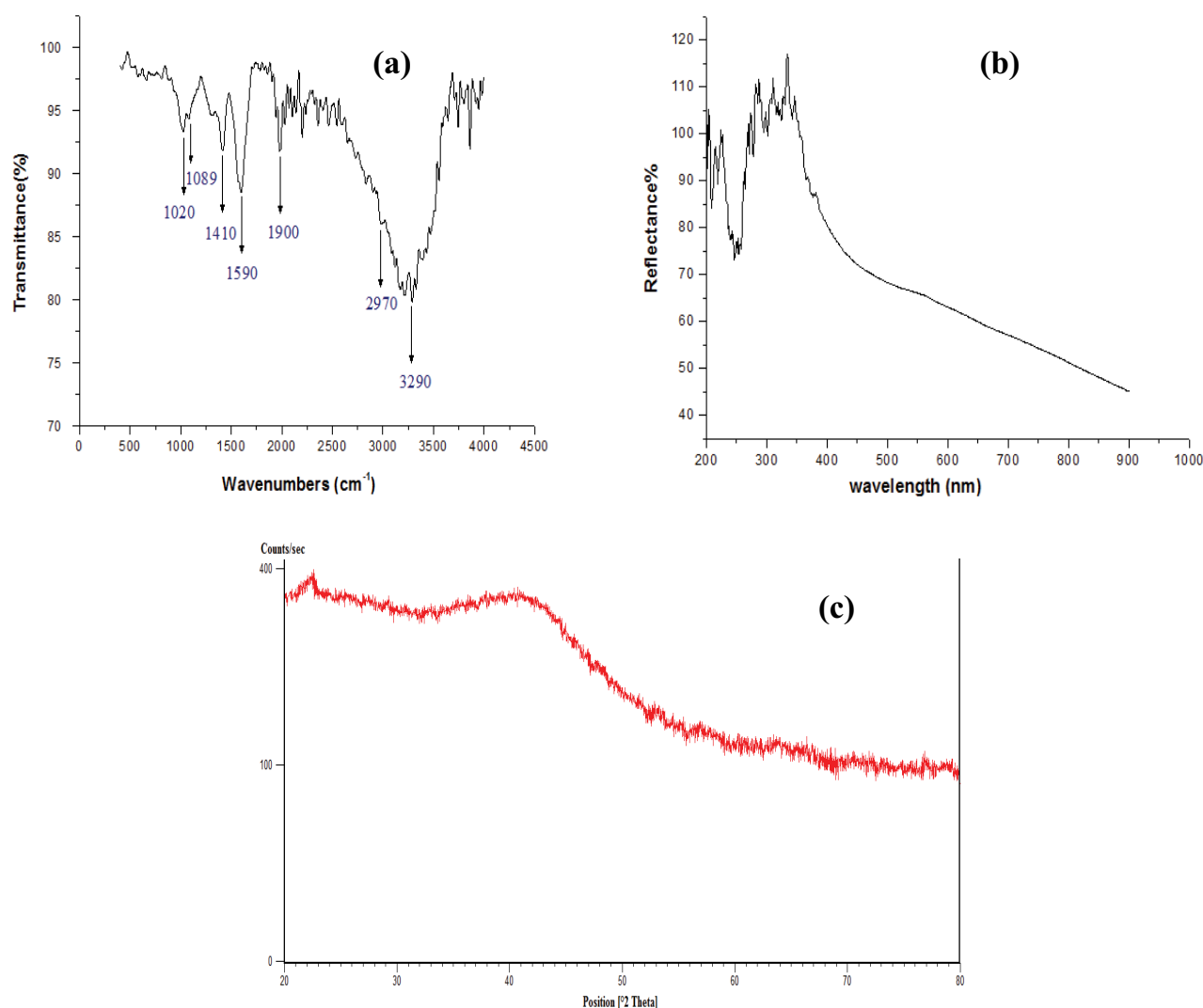


Fig. 3. (a) Fourier-transform infrared spectra, (b) UV-Vis DR spectra and (c) X-ray diffraction pattern of calcium alginate beads.

agreement with the XRD standard of the calcium alginate beads reported previously [13,16].

The surface of this biosorbent was characterized using the results of N_2 adsorption–desorption isotherms (figure not displayed). Based on the Brunauer–Emmett–Teller method, the specific surface area S_{BET} was found to be $18.673 \text{ m}^2/\text{g}$. Total volume pore (V_p) and the average pore diameter were determined by Barrett–Joyner–Halenda method and their values are $0.001046 \text{ cm}^3/\text{g}$ and 18.87 nm , respectively. Results indicate that the adsorbent is a mesoporous material according to pore size classification of International Union of Pure and Applied Chemistry.

UV-Vis diffuse spectra of calcium alginate (Fig. 3b) displays two characteristic absorption bands at 284 and at 385 nm owing to the strong interactions between sodium alginate and the bivalent cations (Ca^{2+}) to obtain the “egg-box” model during the cross-linking process [17].

3.1. Preliminary study of AO dye adsorption

The pre-optimization of the experimental parameters was carried out in this part by changing a single parameter at each study and maintaining the other parameters stable.

3.1.1. Effect of contact time

To establish the optimal contact time for achieving maximum AO dye removal from the aqueous solution, adsorption experiments were conducted. These experiments involved using an initial Auramine O dye concentration of 5 mg/L and 0.1 g of calcium alginate beads (Fig. 4) for duration of 5 h at room temperature. The results indicated that the ideal contact time for maximum removal was 180 min , which was subsequently employed as a constant throughout the entire study.

Furthermore, the experiments demonstrated that dry beads exhibited higher efficiency, achieving a 50% AO removal rate compared to wet beads, which only reached a 33% dye removal rate. As a result, for the remainder of the study, dry calcium alginate beads were utilized as the adsorbent, and the process duration was maintained at 180 min .

3.1.2. Effect of adsorbent dose

As we know the adsorbent dose affects directly the number of binding free sites to absorb the pollutant molecules,

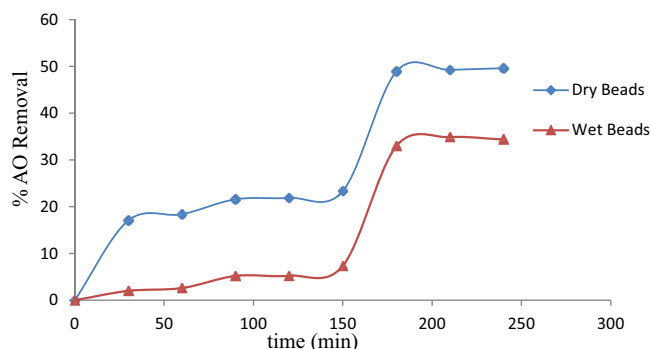


Fig. 4. Effect of contact time for Auramine O removal by dry and wet calcium alginate beads.

several experiments were carried out to study the effect of alginate calcium beads dose on the removal efficiency of AO dye. For these experiments, Erlenmeyer flask containing an initial concentration of 5 mg/L of Auramine O dye was agitated for 180 min at room temperature, with varying adsorbent doses from 25 to 500 mg . The influence of adsorbent dose on the removal efficiency of Auramine O dye is displayed in Fig. 5a. As we can see the increase in adsorbent mass from 25 to 100 mg leads to enhancing the Auramine O dye adsorption to achieve 45% . This is owing to the availability of a large surface area and the existence of more free active sites [18]. Furthermore, increasing the dose of calcium alginate beads above 100 mg causes a significant decrease in AO removal efficiency from 45% to 29% . This can be explained by the reducing in the adsorbate/adsorbent ratio leading to the saturation of available adsorption sites so the increase of beads dose will prevent better removal efficiency [19].

3.1.3. Effect of initial concentration

Fig. 5b shows the effect of initial concentration of AO dye on the removal efficiency using 0.1 g of calcium alginate, $\text{pH } 5$ with a contact time of 180 min and varying the pollutant concentration from 5 to 50 mg/L . Results show that the removal efficiency is strongly affected by varying the initial concentration of dye; it decreases from 58% to 48.16% by increasing the initial dye concentration from 5 to 50 mg/L after being stable (58%) at the concentration range from 5 to 25 mg/L . It is very common and reported previously in many works that by increasing initial concentration of the pollutant, the number of available active sites decreases until reaching saturation which contributes to removal efficiency reduce [20].

3.1.4. Effect of pH

pH plays a significant factor in the adsorption processes by affecting directly the charge in the surface of the adsorbent and the ionization degree of the functional groups on the adsorbent as well and influence the adsorption capacity as a result [21]. The experiment was carried out by studying the dye adsorption over a pH range of 2 – 12 when the other parameters such contact time; dye concentration and alginate dose remain constant at 180 min , 5 mg/L and $0.1 \text{ g}/50 \text{ mL}$, respectively. Fig. 5c shows that the best percentage removal of AO dye is 53.5% which was reached at pH range between 4 and 6 . In basic pH , Auramine O removal percentage decreases to 28.4% at $\text{pH} = 12$ which can be explained by the existence of hydroxide ions (OH^-) in the aqueous solution that leads to a competition with dye. So, increasing the pH solution from 5 to 12 inhibits the adsorption process. This supports the probability that the adsorption mechanism based on the interaction between the ($-$) charge of functional groups (RCOO^-) of the adsorbent and the ($+$) charge of Auramine O dye.

3.1.5. Adsorption isotherms

Adsorption isotherms are crucial to describe the adsorbate interactions with the adsorbent. In this study, the

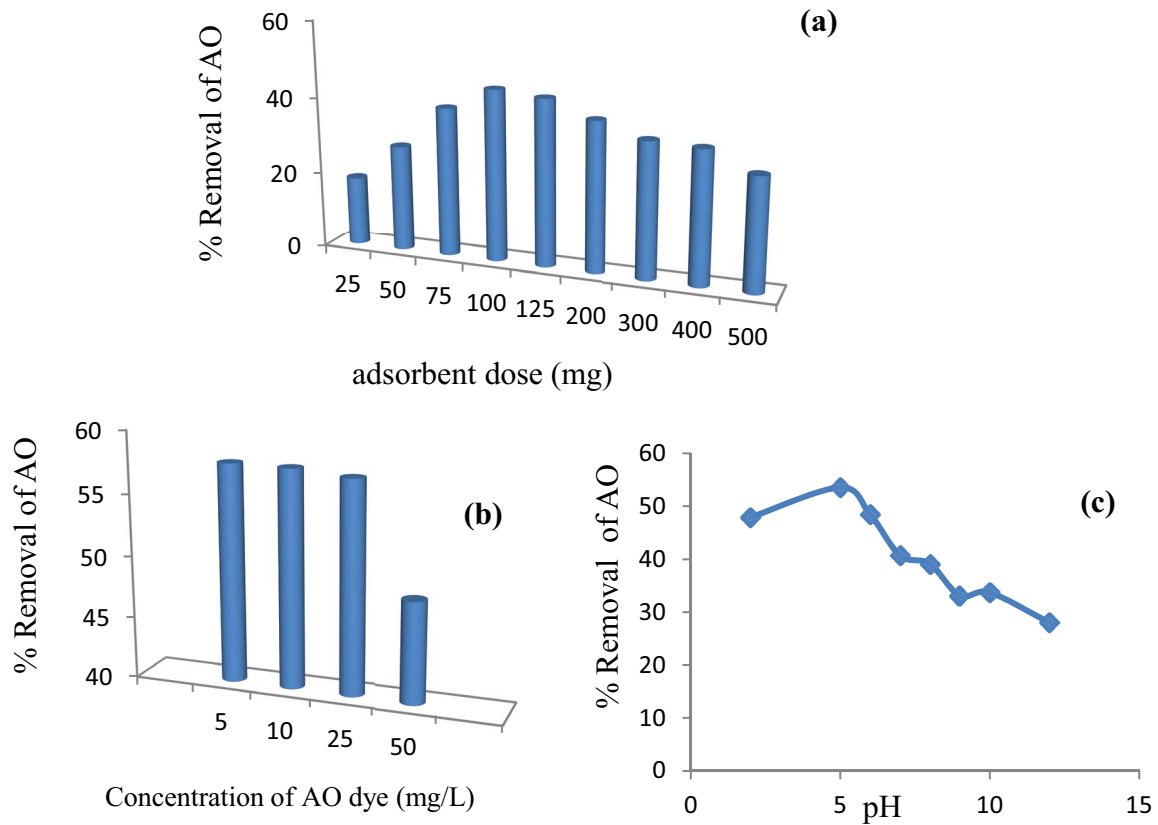


Fig. 5. Effect of: (a) adsorbent dose, (b) initial concentration, and (c) pH on Auramine O removal.

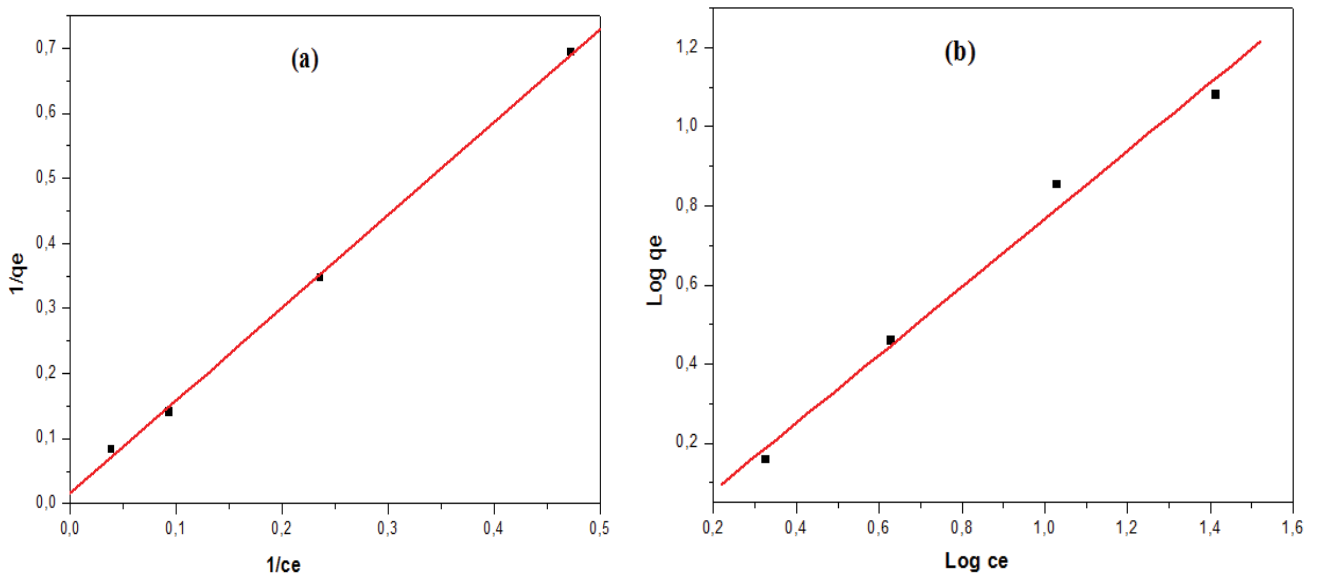


Fig. 6. Adsorption isotherm of Auramine O onto calcium alginate beads: (a) Langmuir and (b) Freundlich models.

Langmuir and Freundlich isotherms were selected. Results (Fig. 6 and Table 1) show that Langmuir model fits well with experimental data ($R^2 = 0.999$), suggesting that adsorption process of AO dye on the surface sites of the beads is monolayer.

3.1.6. Kinetic modeling

Pseudo-first-order and pseudo-second-order models are usually used as linear equations to explain kinetics adsorption and the adsorption mechanism process. In addition to

that, the correlation coefficients are the main indicators to the compatibility predicted values between experimental data and the models. Results exhibit that pseudo-second-order fits well with experimental data (Fig. 7 and Table 1), since the correlation coefficient value (R^2) is 0.993, suggesting the chemisorption process of Auramine O onto calcium alginate beads [22,23].

3.2. Preliminary study of phosphate adsorption

3.2.1. Effect of pH

It is well known that the pH of adsorbate solution is an important factor in adsorption process. Thus, it is

essential to determine from the beginning the optimum pH to adsorb the maximum amount of phosphate.

In order to study the influence of pH on the removal of phosphate, adsorption tests of phosphate onto calcium alginate beads were performed at room temperature under constant conditions including: 10 mg/L of phosphate initial concentration, 1.5 g of calcium alginate beads mass and 180 min of contact time yet varying the pH from 4 to 13.

Fig. 8a shows that pH is an important parameter that affects significantly the phosphate speciation in an aqueous solution and the adsorption process in consequence [24]. As we can see in pH range from 4 to 10, phosphates removal was hardly increasing but it is still very low owing

Table 1 Isotherm and kinetic parameters for the Auramine O dye adsorption onto calcium alginate beads

(a) Langmuir and Freundlich parameters						
Langmuir				Freundlich		
$\frac{1}{q_e} = \left(\frac{1}{K_L \cdot q_{max}} \right) \frac{1}{C_e} + \frac{1}{q_{max}}$ (2)				$\log q_e = \frac{1}{n} \log C_e + \log K_F$ (3)		
q_{max} (mg/g)	K_L (L/mg)	R_L	R^2	K_f (L/mg)	$1/n$	R^2
59.630	0.0117	0.9444	0.999	0.809	0.859	0.993
(b) Kinetic parameters						
Pseudo-first-order model			Pseudo-second-order model			
$\ln(q_e - q_t) = \ln q_e - K_1 t$ (4)			$\frac{t}{q_t} = \frac{1}{K_2 q_e^2} + \frac{1}{q_e} t$ (5)			
q_e (mg/g)	K_1 (min^{-1})	R^2	q_e (mg/g)	K_2 (g/mg·min)	R^2	
1.303	-3.311	0.693	0.673	0.0311	0.993	

q_e : amount of Auramine O adsorbed at equilibrium (mg/g); q_t : amount of Auramine O adsorbed at time t (mg/g); K_1 : rate constant of pseudo-first-order (min^{-1}); K_2 : rate constant of pseudo-second-order (g/mg·min); q_{max} : maximum adsorption capacity (mg/g); C_e : amount of residual dye at equilibrium (mg/L); K_L : Langmuir constant (L/mg); K_f : Freundlich constant; n is an indicator of adsorption effectiveness.

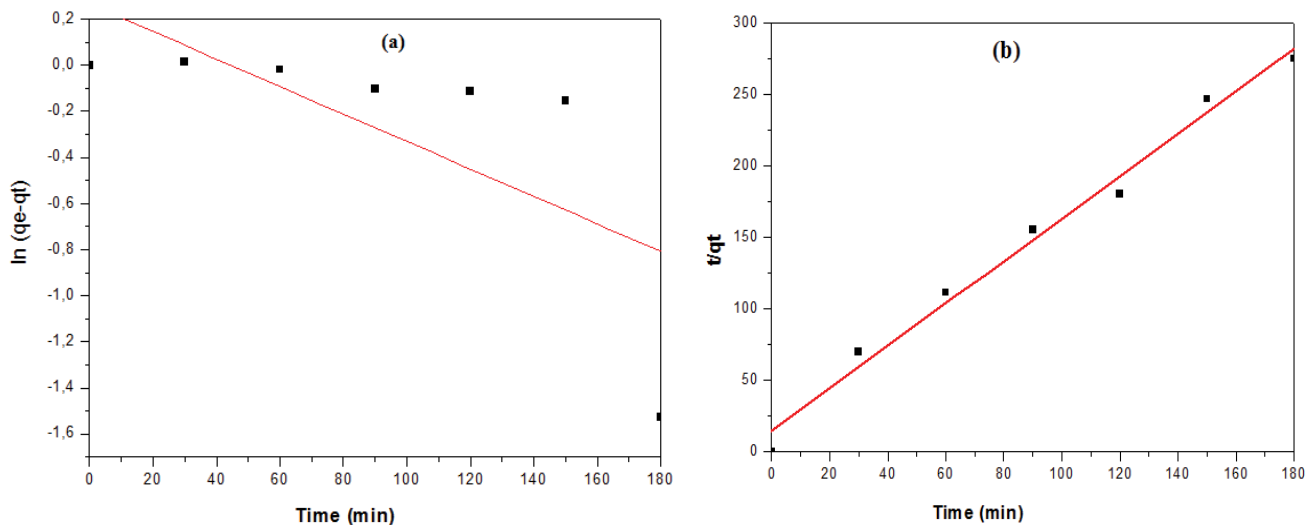


Fig. 7. Kinetic study for Auramine O adsorption onto calcium alginate beads: (a) pseudo-first-order and (b) pseudo-second-order models.

to $H_2PO_4^-$ and HPO_4^{2-} ions existing in the solution at that pH range. The optimum pH value was found to be 12 which gives a maximum phosphate removal (81%), knowing well the presence of PO_4^{3-} species in this high pH [5].

It is worth noting that above pH 12 the phosphate removal reduced to 28% as a result of the competition between OH^- and PO_4^{3-} ions. So, pH 12 has been chosen as an optimum pH for the rest of adsorption tests.

3.2.2. Effect of adsorbent dose

To investigate the impact of adsorbent mass on phosphate adsorption, experiments were performed with an initial phosphate concentration of 10 mg/L at pH 12 and varying adsorbent mass from 0.5 to 2 g. Results (Fig. 8b) show the enhancement of phosphate removal percentage from 73% to 97% by increasing the adsorbent dose from 0.5 to 2 g and that can be related to the existence of more vacancies free active sites on the adsorbent surface. It has been concluded that 2 g of calcium alginate beads is the adequate amount to reach a maximum removal of phosphate.

3.2.3. Effect of initial phosphate concentration

The influence of initial concentration on phosphate adsorption onto calcium alginate beads was studied through a series of experiments at pH 12 using 1.5 g of beads at room temperature and varying the initial concentration from 1 to 10 mg/L. The curve displayed in Fig. 8c shows that phosphate removal percentage increased as the initial concentration increased. This can be explained by the fact that increasing the initial concentration makes

the mass transfer driving force larger leading to higher phosphate adsorption [25].

3.2.4. Adsorption isotherms and kinetic modeling

As can be seen in (Fig. 9 and Table 2), Freundlich model fits better with experimental data ($R^2 = 0.988$) of phosphate onto the beads, suggesting that adsorption process relate, probably, multilayer adsorption with reaction among phosphate molecules and the active site on the beads surface. Kinetic study (Fig. 10 and Table 2) exhibit that the experimental data follows well the pseudo-second-order model with correlation coefficient value (R^2) equal to 0.995 which suggests the chemisorption process of phosphate onto calcium alginate beads.

3.3. Full factorial design for adsorption of AO dye and phosphate

A full study of the influence of all experimental parameters on the adsorption of (AO dye/phosphate) process and their optimization was made using NEMROWD Software, three main factors were chosen. A two-level full factorial design 2^k was performed to investigate the impact of these factors and their interaction on the removal of (AO dye/phosphate) by adsorption onto calcium alginate beads with the limit values of the parameters defined in Table 3. The experimental response associated to a 2^k factorial design (for three variables) is described by a polynomial model of the following form:

$$Y\% = b_0 + b_1X_1 + b_2X_2 + b_3X_3 + b_{12}X_1X_2 + b_{13}X_1X_3 + b_{23}X_2X_3 + B_{123}X_1X_2X_3 \tag{6}$$

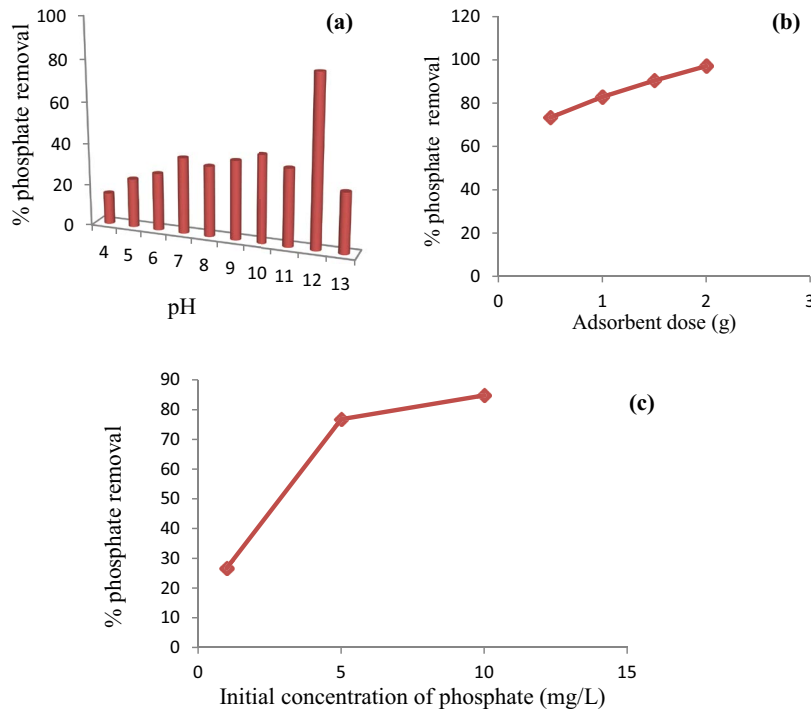


Fig. 8. Influence of parameters on phosphate removal: (a) pH, (b) adsorbent dose, and (c) initial concentration of phosphate solution.

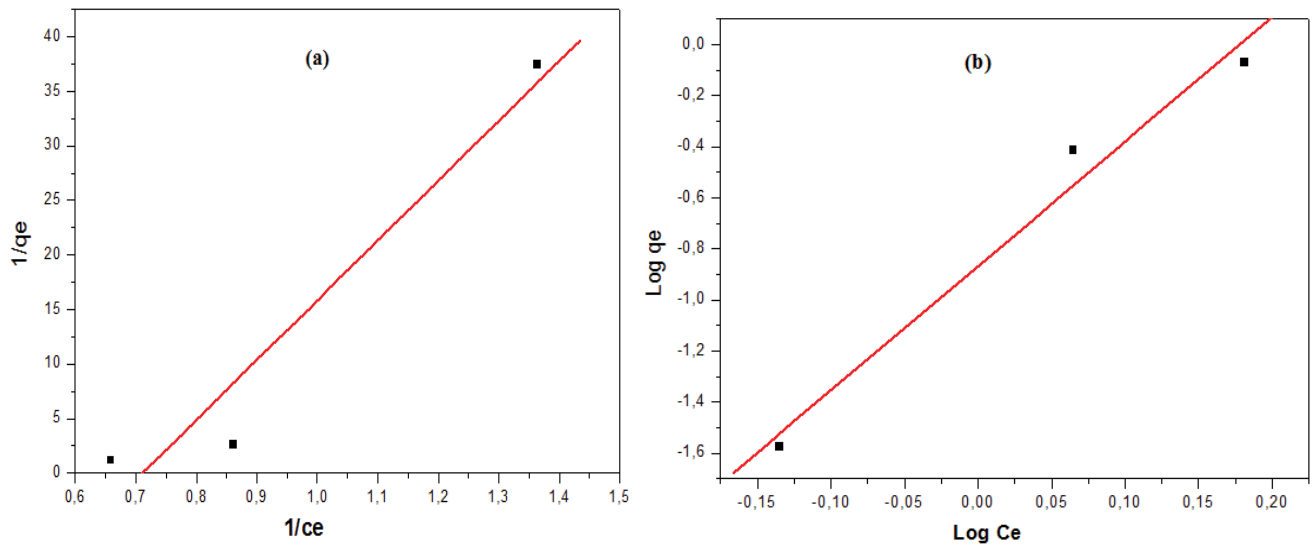


Fig. 9. Adsorption isotherm of phosphate onto calcium alginate beads: (a) Langmuir and (b) Freundlich models.

Table 2
Isotherm and kinetic parameters for the phosphate adsorption onto calcium alginate beads

(a) Langmuir and Freundlich parameters						
Langmuir				Freundlich		
$\frac{1}{q_e} = \left(\frac{1}{K_L \cdot q_{max}} \right) \frac{1}{C_e} + \frac{1}{q_{max}} \quad (2)$				$\log q_e = \frac{1}{n} \log C_e + \log K_F \quad (3)$		
q_{max} (mg/g)	K_L (L/mg)	R_L	R^2	K_F (L/mg)	$1/n$	R^2
0.0256	8.011	0.0123	0.970	4.864	4.864	0.988
(b) Kinetic parameters						
Pseudo-first-order model			Pseudo-second-order model			
$\ln(q_e - q_t) = \ln q_e - K_1 t \quad (4)$			$\frac{t}{q_t} = \frac{1}{K_2 q_e^2} + \frac{1}{q_e} t \quad (5)$			
q_e (mg/g)	K_1 (min ⁻¹)	R^2	q_e (mg/g)	K_2 (g/mg·min)	R^2	
0.638	-5.679	0.974	0.863	0.037	0.995	

where Y : the experimental response (percentage removal); X_i : the coded variable (1 or -1); b_i : the estimation of the principal effect of the factor i for the response Y ; b_{ij} : the estimation of the interaction effect between parameters i and j for the response Y .

Table 3 summarizes the experimental field that used to calculate the coefficients of the Eq. (6).

Based on the experimental results from Tables 4 and 5, the coefficients of the polynomial model were calculated using the NEMROWD Software.

$$Y(\text{AO}\%) = 18.5 - 8.3X_1 + 6.91X_2 + 2.19X_1X_2 + 0.56X_1X_3 + 0.41X_1X_2X_3 \quad (7)$$

$$Y(\text{phosphate}\%) = 48.61 + 20.89X_1 + 6.91X_2 + 2.19X_1X_2 + 0.56X_1X_3 + 0.41X_1X_2X_3 \quad (8)$$

Fig. 11 shows the effects and interactions of the different investigated parameters based on the different coefficients of the polynomial model [Eqs. (7) and (8)] calculated by NEMROWD.

For AO dye adsorption, only two studied parameters had a positive impact on the response which means increasing them causes the enhancement of the Auramine O dye removal. Those factors are pH of the solution and the dose of alginate beads. Meanwhile, initial concentration of the adsorbate had a strong negative impact on the response of AO dye removal.

For phosphate adsorption onto calcium alginate beads, all the three investigated factors had a positive effect on the response which means that increasing the parameters causes the increase in the phosphate removal. Thus, the initial concentration has a significant contribution (88.3%) on the response. So, initial concentration of the pollutant

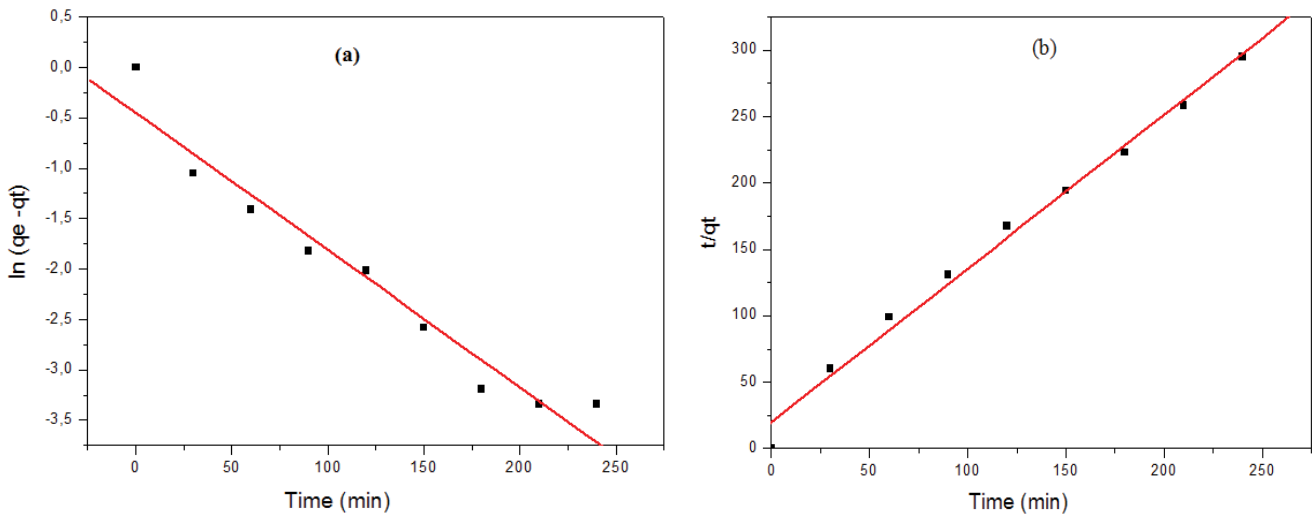


Fig. 10. Kinetic study for phosphate adsorption onto calcium alginate beads: (a) pseudo-first-order and (b) pseudo-second-order models.

Table 3
Experimental area of the studied factors for Auramine O dye/phosphate removal

Variable symbol	Experimental field for Auramine O dye removal		Experimental field for phosphate removal		
	-1	+1	-1	+1	
Initial concentration of (Auramine O/phosphate) mg/L	X_1	5	25	1	10
pH	X_2	5	7	10	12
Dose of calcium alginate beads (g)	X_3	0.025	0.1	0.5	1.5

Table 4
Full factorial design matrix with experimental values for the removal efficiency of Auramine O dye

	X_1	[C]	X_2	pH	X_3	D (g)	Y_{AO} (%)
1	-1	5	-1	5	-1	0.025	18.2
2	+1	25	-1	5	-1	0.025	6.55
3	-1	5	+1	7	-1	0.025	17.46
4	+1	25	+1	7	-1	0.025	8
5	-1	5	-1	5	+1	0.1	48
6	+1	25	-1	5	+1	0.1	36
7	-1	5	+1	7	+1	0.1	35
8	+1	25	+1	7	+1	0.1	17.24

Table 5
Full factorial design matrix with experimental values for the removal efficiency of phosphate

	X_1	[C]	X_2	pH	X_3	D (g)	Y_p (%)
1	-1	1	-1	10	-1	0.5	22
2	+1	10	-1	10	-1	0.5	59
3	-1	1	+1	12	-1	0.5	30
4	+1	10	+1	12	-1	0.5	74
5	-1	1	-1	10	+1	1.5	24
6	+1	10	-1	10	+1	1.5	61.7
7	-1	1	+1	12	+1	1.5	34.4
8	+1	10	+1	12	+1	1.5	82.5

could be deemed as the only parameter that really has an impact on the removal of phosphate.

3.4. Comparison with the results of other bio-sorbents existing in the literature

If we compare the findings achieved under optimum conditions with those already published using different bio-sorbents (Table 6), it is very obvious that calcium alginate beads are considered as competitive adsorbent in terms of removal efficiency of both phosphate and dye.

4. Conclusion

A green, eco-friendly and low-cost calcium alginate beads were fabricated by cross-linking the hydroxyl and carboxyl groups existing in the sodium alginate and the Ca^{2+} of the gelling agent $CaCl_2$. The obtained beads were investigated as an adsorbent to remove Auramine O dye and phosphate from aqueous solution. The characterization study proves that this biopolymer has a great potential to be an efficient adsorbent for pollutants removal. Surface specific area of the beads was found to be 18.673 m^2/g and

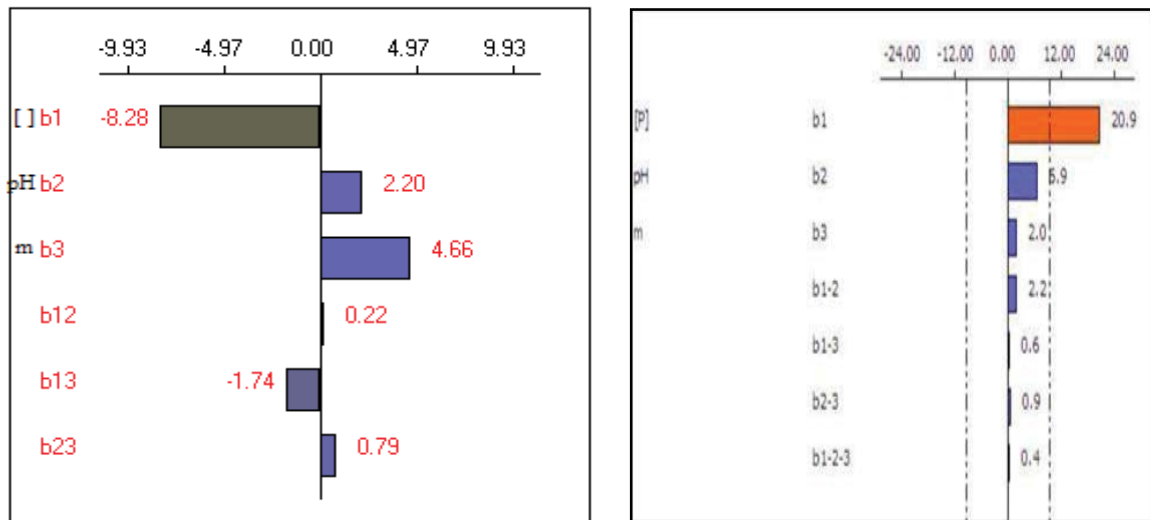


Fig. 11. Graphical analysis of average effects of parameters on adsorption of (a) Auramine O dye and (b) phosphate.

Table 6
Comparison with the results of different natural adsorbents available in the literature

Adsorbent	% phosphate removal	References	% dye removal	References
Date palm waste	87	[26]	98 (dye: Crystal violet)	[27]
Oyster shell powder	48	[28]	100 (dye: Acid green 25)	[29]
Rice husk	83.8	[30]	100 (dye: Methylene blue)	[31]
Calcium alginate beads	82.5	This work	48 (dye: Auramine O)	This work

average pore diameter 18.87 nm which suggests that this green adsorbent is a mesoporous material. Based on the full factors design, AO dye removal by adsorption onto calcium alginate beads was mainly and positively affected by alginate dose and it reached 48% under these optimal conditions: 5 mg/L of initial concentration, 0.1 g of alginate dose and pH 5. For phosphate removal, the initial concentration of phosphate in the solution was proved to have the biggest influence on the phosphate removal by adsorption onto calcium alginate beads leading to the highest percentage removal 82.5%.

Langmuir model fits well with experimental data of AO dye removal ($R^2 = 0.999$), suggesting that adsorption process of Auramine O dye on the surface sites of the beads is monolayer, however for phosphate the adsorption process is multilayer since the experimental related adsorption data fit well with the Freundlich model ($R^2 = 0.988$). Furthermore, the kinetic study reveals that the experimental data closely conforms to the pseudo-second-order model, suggesting that the adsorption process of these adsorbates onto calcium alginate beads is primarily a chemisorption process.

Acknowledgement

The authors extended their appreciation to the Researchers Supporting Project number (RSP 2023R75), King Saudi University, Riyadh Saudi Arabia.

Disclosure statement

The authors report there are no competing interests to declare.

References

- [1] V.J. Vilar, C.M. Botelho, R.A. Boaventura, Equilibrium and kinetic modelling of Cd(II) biosorption by algae *Gelidium* and agar extraction algal waste, *Water Res.*, 40 (2006) 291–302.
- [2] K. Hunger, *Industrial Dyes: Chemistry, Properties, Applications*, John Wiley & Sons, 2007.
- [3] A. Asfaram, M. Ghaedi, S. Hajati, M. Rezaeinejad, A. Goudarzi, M.K. Purkait, Rapid removal of Auramine-O and Methylene blue by ZnS: Cu nanoparticles loaded on activated carbon: a response surface methodology approach, *J. Chem. Eng.*, 53 (2015) 80–91.
- [4] M. Kumar, G. Vijayakumar, R. Tamilarasan, Synthesis, characterization and experimental studies of nano Zn–Al–Fe₃O₄ blended alginate/Ca beads for the adsorption of Rhodamine B, *J. Polym. Environ.*, 27 (2019) 106–117.
- [5] K. Karageorgiou, M. Paschalis, G.N. Anastassakis, Removal of phosphate species from solution by adsorption onto calcite used as natural adsorbent, *J. Hazard. Mater.*, 139 (2007) 447–452.
- [6] S. Wang, Y. Boyjoo, A. Choueib, Z.H. Zhu, Removal of dyes from aqueous solution using fly ash and red mud, *Water Res.*, 39 (2005) 129–138.
- [7] A. Nussinovitch, *Hydrocolloid Applications: Gum Technology in the Food and Other Industries*, Blackie Academic & Professional, London, 1997, pp. 134–137.
- [8] M. Askarieh, H. Farshidi, A., Rashidi, A. Pourreza, M.S. Alivand, Comparative evaluation of MIL-101(Cr)/calcium alginate composite beads as potential adsorbents for removing

- water vapor from air, Sep. Purif. Technol., 291 (2022) 120830, doi: 10.1016/j.seppur.2022.120830.
- [9] C. Gok, S. Aytas, Biosorption of uranium(VI) from aqueous solution using calcium alginate beads, J. Hazard. Mater., 168 (2009) 369–375.
- [10] T.Y. Kim, H.J. Jin, S.S. Park, S.J. Kim, S.Y. Cho, Adsorption equilibrium of copper ion and phenol by powdered activated carbon, alginate bead and alginate-activated carbon bead, J. Hazard. Mater., 14 (2008) 714–719.
- [11] J. Rodier, L'analyse de l'eau, Edition Dunod, Paris, 2009.
- [12] M. Monier, D.A., Abdel-Latif, H.A. Mohammed, Synthesis and characterization of uranyl ion-imprinted microspheres based on amidoximated modified alginate, Int. J. Biol. Macromol., 75 (2015) 354–363.
- [13] S.B. Hammouda, N. Adhoum, L. Monser, Synthesis of magnetic alginate beads based on Fe₃O₄ nanoparticles for the removal of 3-methylindole from aqueous solution using Fenton process, J. Hazard. Mater., 294 (2015) 128–136.
- [14] A. Manuja, S. Kumar, N. Dilbaghi, G. Bhanjana, M. Chopra, H. Kaur, R. Kumar, B.K. Manuja, S.K. Singh, S.C. Yadav, Quinapyramine sulfate-loaded sodium alginate nanoparticles show enhanced trypanocidal activity, Nanomedicine (Lond), 9 (2014) 1625–1634.
- [15] P. Khajavi, A.R. Keshtkar, M.A. Moosavian, The optimization of U(VI) removal by a novel amidoximated modified calcium alginate gel bead with entrapped functionalized SiO₂ nanoparticles, Prog. Nucl. Energy, 140 (2021) 103887, doi: 10.1016/j.pnucene.2021.103887.
- [16] T.H. Wu, F.L. Yen, L.T. Lin, T.R. Tsai, C.C. Lin, T.M. Cham, Preparation, physicochemical characterization, and antioxidant effects of quercetin nanoparticles, Int. J. Pharm., 346 (2008) 160–168.
- [17] A. Djelad, A. Mokhtar, A. Khelifa, A. Bengueddach, M. Sassi, Alginate-whey an effective and green adsorbent for crystal violet removal: kinetic, thermodynamic and mechanism studies, Int. J. Biol. Macromol., 139 (2019) 944–954.
- [18] A.A. Oladipo, M. Gazi, Enhanced removal of crystal violet by low-cost alginate/acid activated bentonite composite beads: optimization and modelling using non-linear regression technique, J. Water Process Eng., 2 (2014) 43–52.
- [19] D.L. Nunes, A.S. Franca, L.S. Oliveira, Use of *Raphanus sativus* L. press cake, a solid residue from biodiesel processing, in the production of adsorbents by microwave activation, Environ. Technol., 32 (2011) 1073–1083.
- [20] C.I. Covaliu, G. Paraschiv, O. Stoian, A. Vişan, Nanomaterials applied for heavy metals removal from wastewater, IOP Conf. Ser.: Mater. Sci. Eng., 572 (2019) 012074, doi: 10.1088/1757-899X/572/1/012074.
- [21] A.Ü. Metin, D. Doğan, M. Can, Novel magnetic gel beads based on ionically crosslinked sodium alginate and polyanetholesulfonic acid: synthesis and application for adsorption of cationic dyes, Mater. Chem. Phys., 256 (2020) 123659, doi: 10.1016/j.matchemphys.2020.123659.
- [22] C. Muthukumar, V.M. Sivakumar, S. Sumathi, M. Thirumari-murugan, Adsorptive removal of recalcitrant Auramine-O dye by sodium dodecyl sulfate functionalized magnetite nanoparticles: isotherm, kinetics, and fixed-bed column studies, Int. J. Nanosci., 19 (2020) 1793–5350.
- [23] C. Qi, M. Meng, Q. Liu, C. Kang, S. Huang, Z. Zhou, C. Chen, Adsorption kinetics and thermodynamics of auramine-O on sugarcane leaf-based activated carbon, J. Dispersion Sci. Technol., 36 (2015) 1257–1263.
- [24] S. Sudhakaran, E.V. Abraham, H. Mahadevan, K.A. Krishnan, Crosslinked chitosan-montmorillonite biocomposite with Fe intercalation: enhancing surface chemistry for improved phosphate adsorption, Surf. Interfaces, 27 (2021) 101468, doi: 10.1016/j.surfin.2021.101468.
- [25] N. Nasuha, B.H. Hameed, A.T.M. Din, Rejected tea as a potential low-cost adsorbent for the removal of methylene blue, J. Hazard. Mater., 175 (2010) 126–132.
- [26] Z.Z. Ismail, Kinetic study for phosphate removal from water by recycled date-palm wastes as agricultural by-products, Int. J. Environ. Sci. Technol., 69 (2012) 135–149.
- [27] M. Alshabanat, G. Alsenani, R. Almufarij, Removal of crystal violet dye from aqueous solutions onto date palm fiber by adsorption technique, J. Chem., 2013 (2013) 210239, doi: 10.1155/2013/210239.
- [28] C. Namasivayam, A. Sakoda, M. Suzuki, Removal of phosphate by adsorption onto oyster shell powder—kinetic studies, J. Chem. Technol. Biotechnol., 80 (2005) 356–358.
- [29] X. Inthapanya, S. Wu, Z. Han, G. Zeng, M. Wu, C. Yang, Adsorptive removal of anionic dye using calcined oyster shells: isotherms, kinetics, and thermodynamics, Environ. Sci. Pollut. Res., 26 (2019) 5944–5954.
- [30] N. Sooksawat, S. Santibenchakul, M. Kruatrachue, D. Inthorn, Recycling rice husk for removal of phosphate and nitrate from synthetic and swine wastewater: adsorption study and nutrient analysis of modified rice husk, J. Environ. Sci. Health. Part A Toxic/Hazard. Subst. Environ. Eng., 56 (2021) 1080–1092.
- [31] X.G. Chen, S.S. Lv, S.T. Liu, P.P. Zhang, A.B. Zhang, J. Sun, Y. Yue Adsorption of methylene blue by rice hull ash, Sep. Sci. Technol., 47 (2012) 147–156.